Deletional Tolerance Mediated by Extrathymic Aire-Expressing Cells

James M. Gardner, *et al.*

Science **321**, 843 (2008);
DOI: 10.1126/science.1159407

Science (print ISSN 0036-8075; online ISSN 1095-9203) is published weekly, except the last week in December, by the American Association for the Advancement of Science, 1200 New York Avenue NW, Washington, DC 20005.

14. H. Wegmeyer *et al.*, *Neuron* **55**, 756 (2007).
15. A. A. Beg, J. E. Sommer, J. H. Martin, P. Scheiffele, *Neuron* **55**, 768 (2007).
16. L. Shi *et al.*, *Proc. Natl. Acad. Sci. U.S.A.* **104**, 16347 (2007).
17. T. J. Van de Ven, H. M. VanDongen, A. M. VanDongen, *J. Neurosci.* **25**, 9488 (2005).
18. P. Buttery *et al.*, *Proc. Natl. Acad. Sci. U.S.A.* **103**, 1924 (2006).
19. J. M. Dong, P. Smith, C. Hall, L. Lim, *Eur. J. Biochem.* **227**, 636 (1995).
20. C. Hall *et al.*, *Mol. Cell. Biol.* **13**, 4986 (1993).
21. C. Hall *et al.*, *J. Neurosci.* **21**, 5191 (2001).
22. B. Canagarajah *et al.*, *Cell* **119**, 407 (2004).
23. J. K. Chilton, S. Guthrie, *J. Comp. Neurol.* **472**, 308 (2004).
24. J. E. Cooke, C. B. Moens, *Trends Neurosci.* **25**, 260 (2002).
25. S. Guthrie, *Nat. Rev. Neurosci.* **8**, 859 (2007).
26. L. Zhou *et al.*, *J. Neurosci.* **27**, 5127 (2007).
27. M. Sahin *et al.*, *Neuron* **46**, 191 (2005).
28. We dedicate this paper to the memory of Krystal Law, who researched DURS2 in the Engle lab for her undergraduate thesis at Harvard University. We thank the families for their participation, members of the Engle lab for their thoughtful comments, J. Demer for pedigree referral, and M. Gregas, A. Di Nardo, Y. Harada, and I. Eisenberg for technical advice or assistance. Supported by grants from the National Eye Institute (E.C.E.), the Children's Hospital Boston Mental Retardation and Developmental Disabilities Research Center (E.C.E. and M.S.), the Spinal Muscular Atrophy Foundation and American Academy of Neurology (M.S.), South West Regional Development Agency (UK) (J.C. and J.A.), Wellcome Trust (M.C., N.J.G., S.G., S.L., M.P., and E.Y.), Medical Research Council (UK) (M.C., S.G., and S.L.), Clayton Foundation for Research (J.T.S. and B.A.), Research to Prevent Blindness Inc. [J.T.S., B.A., and A.I. (Career Development Award and unrestricted grant to the University of Tennessee Health Science Center, Hamilton Eye Institute)], and Futura-Onlus, Italy (A.B.). E.C.E. is a Howard Hughes Medical Institute Investigator. GenBank accession numbers: human *CHN1* mRNA, NM_001822; mouse *CHN1* mRNA, NM_001113246; chick *CHN1* mRNA, NM_001012952; human α2-chimaerin protein sequence, NP_001813. Protein Data Bank ID: human β2-chimaerin protein sequence, 1XA6.

Supporting Online Material
www.sciencemag.org/cgi/content/full/1156121/DC1
Materials and Methods
Figs. S1 to S8
Table S1
References

5 February 2008; accepted 30 June 2008
Published online 24 July 2008;
10.1126/science.1156121
Include this information when citing this paper.

Deletional Tolerance Mediated by Extrathymic Aire-Expressing Cells

James M. Gardner,[1] Jason J. DeVoss,[1] Rachel S. Friedman,[2] David J. Wong,[3] Ying X. Tan,[1] Xuyu Zhou,[1] Kellsey P. Johannes,[1] Maureen A. Su,[1,4] Howard Y. Chang,[3] Matthew F. Krummel,[2] Mark S. Anderson[1]*

The prevention of autoimmunity requires the elimination of self-reactive T cells during their development and maturation. The expression of diverse self-antigens by stromal cells in the thymus is essential to this process and depends, in part, on the activity of the autoimmune regulator (*Aire*) gene. Here we report the identification of extrathymic *Aire*-expressing cells (eTACs) resident within the secondary lymphoid organs. These stromally derived eTACs express a diverse array of distinct self-antigens and are capable of interacting with and deleting naïve autoreactive T cells. Using two-photon microscopy, we observed stable antigen-specific interactions between eTACs and autoreactive T cells. We propose that such a secondary network of self-antigen–expressing stromal cells may help reinforce immune tolerance by preventing the maturation of autoreactive T cells that escape thymic negative selection.

Immunological tolerance to self is essential in the prevention of autoimmune disease. Mechanisms of central tolerance are mediated in part through the expression of a wide array of otherwise tissue-specific self-antigens (TSAs) such as insulin and thyroglobulin in specialized medullary thymic epithelial cells (mTECs) (*1*–*3*). The thymic expression of many of these TSAs is dependent on the autoimmune regulator (*Aire*) gene (*4*, *5*), and mutations in *Aire* lead to severe, multiorgan, tissue-specific autoimmunity in both mice (*4*, *6*) and humans (*7*, *8*). Although these results reveal a role for thymic *Aire*, self-tolerance must continue to be enforced after T cells leave the thymus. Consistent with this fact, *Aire* expression is also detectable outside the thymus, notably in the secondary lymphoid tissues (*4*, *9*), although the identity and function of such extrathymic *Aire*-expressing cells remain unclear (*10*, *11*). Here we identify a population of extrathymic *Aire*-expressing cells and examine a potential role for *Aire* in maintaining peripheral tolerance.

To accurately label *Aire*-expressing cells in vivo, we employed a bacterial artificial chromosome (BAC) transgenic approach (*12*) using the murine *Aire* locus modified to drive expression of green fluorescent protein (*Gfp*) fused to an autoimmune diabetes-related self-antigen gene, islet-specific glucose-6-phosphatase–related protein (*Igrp*) (Fig. 1A) (*13*). IGRP is a pancreatic β cell–specific protein against which autoreactive CD8 T cells are produced in both mouse and human autoimmune diabetes (*14*–*17*). We elected to include *Igrp* in our transgenic construct because it is not detectable in the thymus (fig. S1A) and because an IGRP-specific T cell receptor (TCR)–transgenic line (*8.3*) (*14*) can be used to monitor interactions of *Igrp-Gfp*–expressing cells. To verify the fidelity of the BAC transgene in recapitulating endogenous *Aire* expression in the resultant *Adig* (*Aire*-driven *Igrp-Gfp*) transgenic mice, thymic sections were co-stained for Aire and GFP, revealing thymic GFP expression highly restricted to *Aire*-expressing cells in the medulla (Fig. 1B and fig. S1B). By flow cytometry, GFP^+ cells were detectable specifically within the mTEC compartment (Fig. 1C), with approximately 30 to 40% of mTECs being GFP-positive. GFP^+ mTECs expressed uniformly high levels of class II major histocompatibility complex (MHC) and CD80 (Fig. 1D), as in previous studies of *Aire*-expressing mTECs (*3*, *11*, *18*).

To test how the introduction of IGRP into the thymic medullary epithelium might affect T cell selection, we compared *8.3* TCR-transgenic and *8.3*/*Adig* double-transgenic mice. Tetramer staining confirmed that the *8.3*/*Adig* double-transgenic mice showed a significant decrease in the percent and avidity of IGRP-specific $CD8^+$ T cells in the thymus (Fig. 1E) and in the periphery (fig. S1C). Further, although IGRP-reactive $CD8^+$ T cells were readily detected in the polyclonal wild-type NOD background, they were completely absent in *Adig* NOD mice (fig. S1D). To test the functional impact of this negative selection, *8.3* and *8.3*/*Adig* mice were followed for diabetes incidence, and *8.3*/*Adig* mice were completely protected from disease (Fig. 1F).

In a broad tissue survey using immunofluorescent anti-GFP staining, expression of the transgene was undetectable in most tissues, but distinct populations of extrathymic transgene-expressing cells were observed within the lymph nodes and spleen (fig. S2A). These extra-thymic *Aire*-expressing cells (eTACs) were generally confined to the T cell zones of the secondary lymphoid organs and preferentially localized to T cell–B cell boundary regions (Fig. 2, A and B). Immunofluorescent co-stains showed these cells to be negative for B cell (B220), fibroblastic reticular cell (gp38 and ERTR-7), and dendritic cell (CD11c) markers, but positive for class II MHC (Fig. 2, A and B). Reciprocal bone-marrow chimeras demonstrated that many of

[1]Diabetes Center, University of California San Francisco (UCSF), San Francisco, CA 94122, USA. [2]Department of Pathology, UCSF, San Francisco, CA 94143, USA. [3]Program in Epithelial Biology, Cancer Biology Program, Stanford University School of Medicine, Stanford, CA 94305, USA. [4]Department of Pediatrics, UCSF, San Francisco, CA 94122, USA.

*To whom correspondence should be addressed. E-mail: manderson@diabetes.ucsf.edu

these cells were stromal in origin (fig. S3A). Given this, we isolated secondary lymphoid stroma by flow cytometry and found that, as in the thymus, a population of GFP$^+$ cells was present that was CD45$^-$, MHC II$^+$ (Fig. 2C). These CD45$^-$ eTACs shared some characteristics with mTECs [being positive for MHC II, programmed death-1 ligand 1, and epithelial cell adhesion molecule (EpCAM)] but were distinct in that eTACs did not express the costimulatory molecules CD80 and CD86 (Fig. 2D). Although GFP$^+$ eTACs represented a significant percentage of the EpCAM$^+$ stromal cells in the periphery (8.5 ±2.4%), eTACs failed to bind the mTEC marker *Ulex europeus* agglutinin I or the fibroblastic reticular cell marker gp38, suggesting that they are distinct from previously described self-antigen–expressing stromal populations (*9*) (fig. S4). eTACs also appeared to be ubiquitous in lymphoid organs, because they were detected in mesenteric lymph nodes, Peyer's patches (fig. S2B), and the tertiary lymphoid structures that form in the infiltrated pancreatic islets of NOD mice (fig. S2C). By flow cytometry, GFP$^+$ cells were also detected in the CD45$^+$ compartment that expressed CD11c, although the level of GFP expression in these cells was significantly lower than in the CD45$^-$ cells and less enriched in *Aire* message (Fig. 2E and fig. S4).

To validate the idea that *Igrp-Gfp* transgene expression in eTACs reflected endogenous *Aire* expression, the eTAC surface markers identified in *Adig* mice (CD45$^-$, MHC II$^+$, EpCAM$^+$) were used to sort eTACs from nontransgenic mice, and *Aire* transcript was indeed found to be abundant in these cells, confirming that this stromal population expressed high levels of *Aire* (Fig. 2E). Co-staining of secondary lymphoid organs for Aire and GFP also showed Aire protein localized to perinuclear speckles within a subset of eTACs (Fig. 2F). The number of GFP$^+$ cells in which Aire protein could be detected was smaller in the periphery (24.8 ± 4.6%) than in the thymus (85.0 ± 4.5%), and the Aire staining was much weaker—near the limit of detection—which may explain why previous attempts to identify these cells in the absence of the transgenic reporter have been difficult (*11*).

Because *Aire* has been shown to play an important role in the transcriptional regulation of self-antigens in mTECs, we sought to define its function as a transcriptional regulator in eTACs. GFP$^+$ eTACs were sorted for microarray analysis from the spleens and pooled lymph nodes of *Adig* mice crossed onto the *Aire*$^{+/+}$ or *Aire*$^{-/-}$ background. As in mTECs, the number of genes up-regulated by *Aire* in eTACs was greater than the number down-regulated (Fig. 3A and tables S1 and S2). Both the total number of *Aire*-regulated genes in eTACs and the fold change of expression of those genes were smaller than has been observed in mTECs, perhaps reflecting the lower and potentially transient expression of *Aire* in the periphery. There was little overlap between *Aire*-regulated genes in eTACs and those in mTECs (Fig. 3B), suggesting that *Aire* in the periphery may regulate the expression of a distinct set of self-antigens. Despite these differences, however, we found a significant enhancement for TSAs among the positively *Aire*-regulated genes in eTACs (Fig. 3C), several of which were confirmed by quantitative reverse transcription polymerase chain

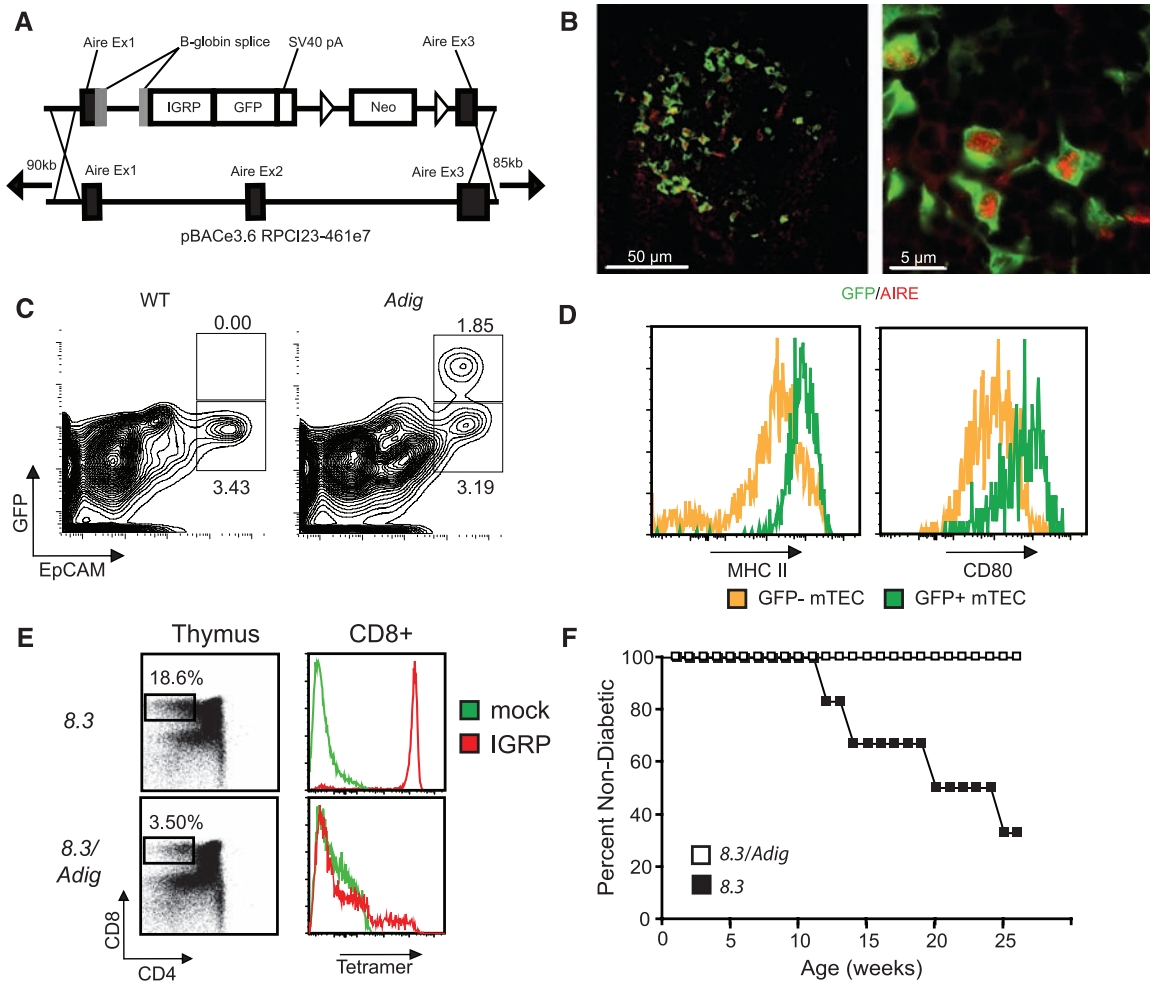

Fig. 1. The *Adig* transgene recapitulates *Aire* expression in the thymus and mediates the negative selection of autoreactive T cells. (**A**) Schematic of *Igrp-Gfp* transgene targeting the *Aire* BAC. Targeting replaces *Aire* exon 2, the coding portion of exon 1, and part of exon 3, so that the transgene does not make functional Aire. (**B**) Immunofluorescent staining of GFP (green) and Aire (red) in thymic frozen sections of *Adig* mice. (**C**) Flow cytometry of CD45-, 4′,6′-diamidino-2-phenylindole– (DAPI-), and Ly51lo-gated thymic stromal cells from wild-type (left) and *Adig* (right) NOD mice. (**D**) Flow cytometry of CD45-, DAPI-, and Ly51lo-gated EpCAM$^+$ mTECs from *Adig* NOD mice gated as GFP$^-$ (yellow) or GFP$^+$ (green) and stained for MHC II (left) and CD80 (right). (**E**) Thymocytes from *8.3* TCR-transgenic mice (top panels) or double-transgenic *8.3/Adig* mice (bottom panels) stained for CD4/CD8 (left panels), or pre-gated as CD4$^-$ CD8$^+$ and stained for IGRP-mimetope (red) or mock (green) peptide/K^d tetramer reactivity (right panels). (**F**) Diabetes incidence curves for *8.3* TCR-transgenic mice (n = 6) and *8.3/Adig* double-transgenic mice (n = 10).

reaction (PCR) (Fig. 3D). The list of genes regulated by *Aire* in eTACs also included a number of self-antigens whose human homologs have been described as autoantigens in human autoimmune diseases, including desmoglein 1a (pemphigus foliaceus) (*19*), ladinin 1 (linear IgA dermatosis) (*20*), and the *N*-methyl-D-aspartate (NMDA) receptor 2C (systemic lupus erythematosis) (*21*). Like other professional antigen-presenting cells (APCs), eTACs also expressed a large number of antigen-processing and presentation genes, suggesting a likely role for T cell interaction (Fig. 3E). Comparison of global gene expression profiles between eTACs, mTECs, cortical thymic epithelial cells (cTECs), thymic dendritic cells (DCs), and macrophages indicated that eTACs were most similar to DCs and mTECs (Fig. 3F).

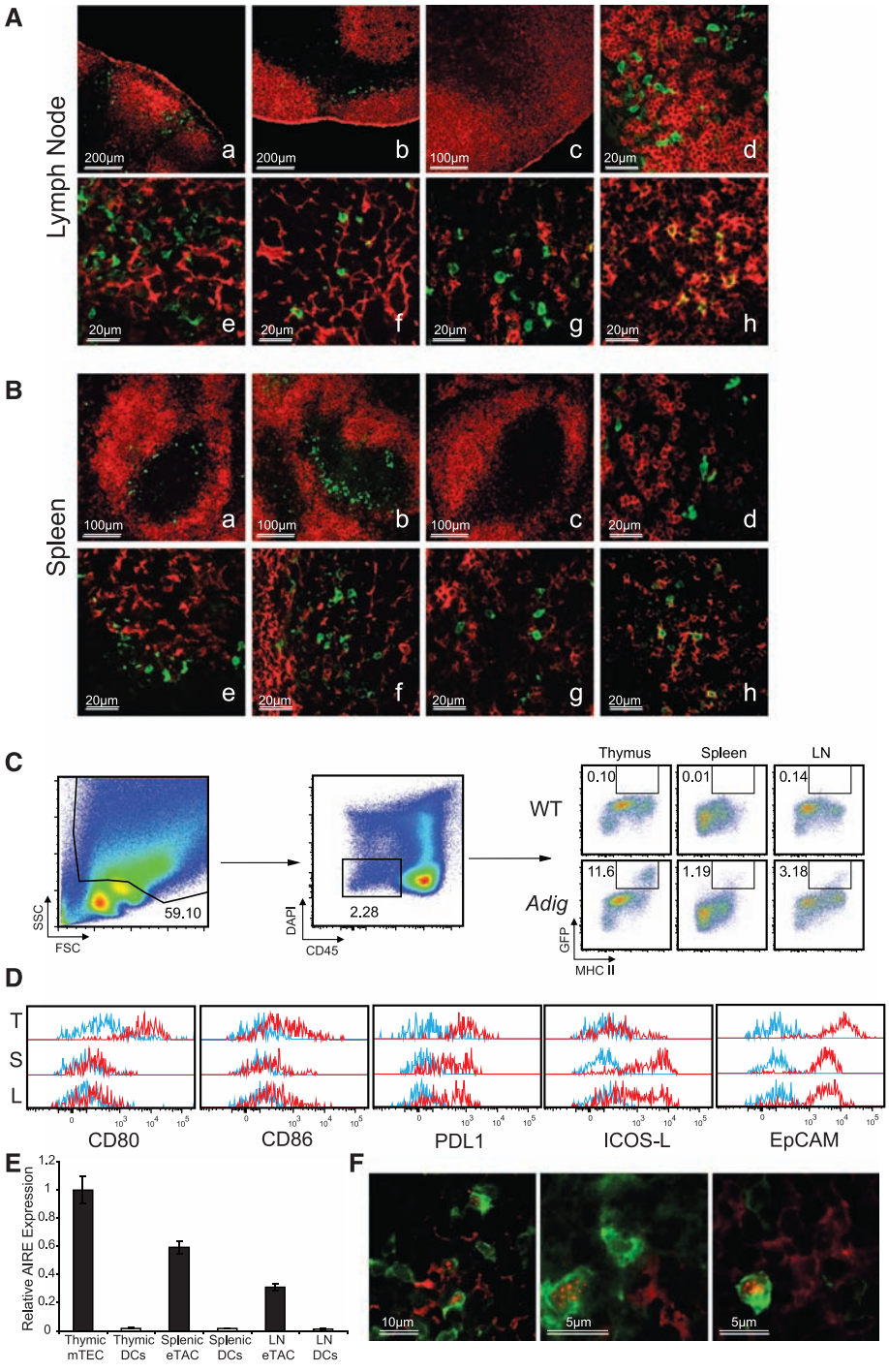

Fig. 2. *Aire*-expressing stromal cells exist in the secondary lymphoid organs. (**A** and **B**) Representative immunofluorescent co-stains of lymph node (A) and spleen (B) sections co-stained for GFP (green, all sections) and B220 (a to d), gp38 (e), ERTR-7 (f), CD11c (g), or MHC II (h; all red). Images a, b, and d to h are from *Adig* NOD mice; images labeled c are from wild-type (WT) NOD mice. (**C**) Flow cytometric analysis and gating from *Adig* and wild-type NOD thymus, spleen, and lymph node stroma analyzed for CD45, DAPI, MHC II, and GFP. (**D**) Flow cytometric analysis of *Adig* NOD thymus (T), spleen (S), and lymph nodes (L), showing expression of indicated markers (red) or isotype staining (blue) in mTECs and eTACs respectively, defined as $CD45^-$, $DAPI^-$, MHC II^+, GFP^+. (**E**) Real-time PCR analysis of *Aire* expression relative to endogenous control in cell-sorted mTECs and eTACs [$CD45^-$, propidium iodide–negative (PI^-), MHC II^+, $CD11c^-$, $EpCAM^+$] and DCs ($CD45^+$, PI^-, MHC II^+, $CD11c^+$, $EpCAM^-$) of nontransgenic NOD thymus, spleen, and lymph node. (**F**) Immunofluorescent GFP (green) and Aire (red) co-stains of lymph nodes from *Adig* NOD mice.

To directly test the ability of eTACs to promote tolerance by interacting with and deleting autoreactive T cells, adoptive co-transfer of carboxyfluorescein diacetate succinimidyl ester (CFSE)–labeled congenic *8.3* and polyclonal $CD8^+$ T cells was used. Upon transfer into wild-type hosts, *8.3* $CD8^+$ T cells proliferated only in the pancreatic lymph nodes and persisted in all lymph nodes for up to 2 weeks (Fig. 4A). When transferred into *Adig* hosts, however, the entire population of *8.3* T cells had proliferated rapidly in all secondary lymphoid organs by 3 days after transfer (Fig. 4A) and had nearly disappeared by 2 weeks after transfer (Fig. 4, A and C). To confirm that the absence of *8.3* T cells in transgenic recipients was due to cell death and not egress, these experiments were repeated in the presence of the S1P1 inhibitor FTY 720 (*22*) (fig. S5). Further, to determine whether a stromal eTAC population was sufficient to directly mediate this deletion, irradiated wild-type and *Adig* mice were reconstituted with bone marrow deficient in β*2-microglobulin* ($\beta2M^{-/-}$), so that only stromal cells were capable of interacting with $CD8^+$ lymphocytes. Chimerism was confirmed both by blood typing and functionally by the observation that *8.3* T cells failed to proliferate in the pancreatic lymph nodes of nontransgenic $\beta2M^{-/-}$ reconstituted mice (Fig. 4B). In contrast, *8.3* T cells continued to proliferate in all secondary lymphoid organs of *Adig* $\beta2M^{-/-}$ reconstituted mice at 3 days, and all divided *8.3* T cells had been deleted by 14 days (Fig. 4, B and C). Although *8.3* cell division was less robust at day 3 in $\beta2M^{-/-}$ chimeric *Adig* mice when compared to unirradiated *Adig* mice, antigen-specific cell death at day 14 was even more dramatic in this setting (Fig. 4, A versus B).

To clearly delineate whether eTACs can directly interact with T cells, two-photon microscopy of explanted lymph nodes was used. GFP^+ cells were observed in all examined lymph nodes of *Adig* mice (movie S1), in a distribution that mirrored the localization of eTACs observed by immunofluorescent staining (movie S2 and Fig. 2A). Adoptive cotransfer of fluorophore-labeled *8.3* and polyclonal $CD8^+$ T cells demonstrated sustained antigen-specific association between naïve *8.3* T cells and eTACs as early as 4 hours after transfer (Fig. 4, D and E, and movies S3 and S4). *8.3* T cells exhib-

ited distinct reductions in speed and total displacement relative to polyclonal CD8$^+$ T cells (Fig. 4, D and F), and *8.3* T cells spent significantly more time both stopped and in direct contact with eTACs (Fig. 4F). Indeed, the upper limit of this interaction time is unknown, as many *8.3* T cells spent the entire 30-min duration of the acquisition periods in continuous contact (Fig. 4G and movie S5). Some GFP$^+$ cells in the lymph node appeared highly motile, but *8.3* T cells were able to maintain antigen-specific interactions despite this motility (Fig. 4E and movie S6). Together, these results suggested that eTACs can form early, stable, long-term contacts with naïve autoreactive T cells entering the lymph node, and that such interaction leads to rapid proliferation and deletion of these T cells.

We have identified a previously unknown population of extrathymic *Aire*-expressing cells (eTACs) that may play an important and previously uncharacterized role in self-tolerance via the deletion of autoreactive T cells. eTACs share certain characteristics with mTECs, including being equipped to act as professional APCs and the Aire-regulated expression of TSAs. The set of Aire-regulated TSAs expressed in eTACs appears to have little overlap with thymic Aire-regulated antigens, which may explain why previous efforts examining known thymic TSAs for expression in secondary lymphoid organs have been inconsistent or conflicting. The lack of overlap suggests that there may be a higher order of Aire-dependent transcriptional regulation of TSA expression, whether direct or indirect, that differs between the thymus and the periphery. Many important questions remain, including the developmental origin of eTACs and their relationship with other possible stromal APC populations (*9*). In this regard, the precise identification of eTACs will provide the framework for exploring these issues. Further, it will be important to determine the physiologic relevance of this cell population in a nontransgenic setting, given the

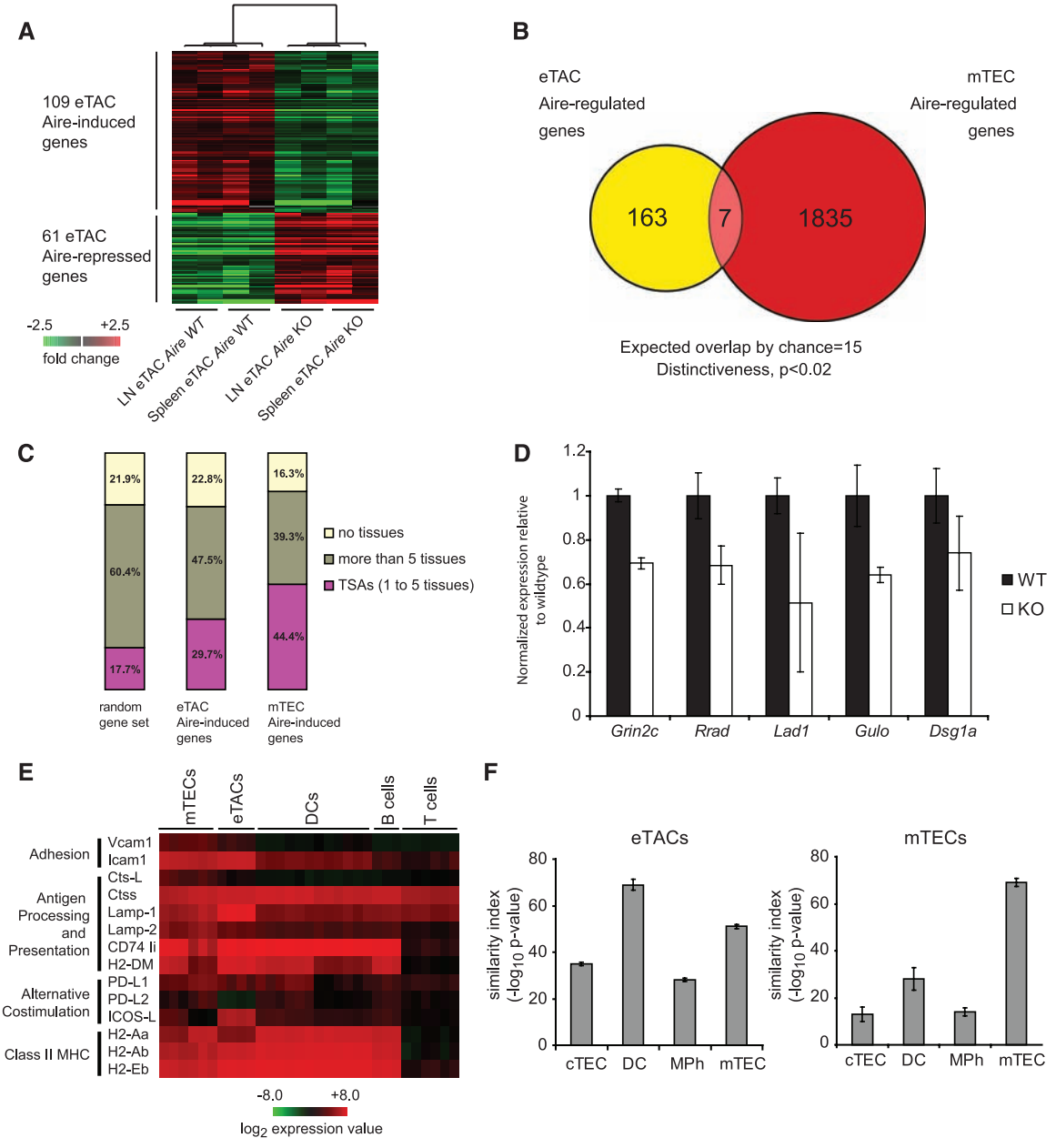

Fig. 3. *Aire* regulates the expression of a set of tissue-specific antigens in eTACs. (**A**) Heat map and unsupervised clustering of *Aire*-regulated genes in eTACs. Pooled eTACs were sorted from lymph nodes and spleens from cohorts of 3- to 6-week-old *Adig Aire*$^{+/+}$ and *Adig Aire*$^{-/-}$ NOD mice. Each of the eight arrays represents three to five pooled mice. (**B**) Schematic diagram of the unshared and common genes regulated by *Aire* in eTACs and mTECs. (**C**) Classification of *Aire*-regulated genes in eTACs based on tissue specificity, as compared to mTECs and to a random gene set. (**D**) Real-time PCR analysis of *Aire*-regulated TSAs in eTACs, normalized to endogenous control. eTACs were sorted from pooled nontransgenic *Aire*$^{+/+}$ [black bars, wild type (WT)] and *Aire*$^{-/-}$ [white bars, knockout (KO)] NOD spleens based on the surface marker profile CD45$^-$, PI$^-$, CD11c$^-$, MHC II$^+$, EpCAM$^+$, and characterized for expression of glutamate receptor NMDA2C (*Grin2c*), Ras-related associated with diabetes (*Rrad*), ladinin 1 (*Lad1*), gulonolactone (L-) oxidase (*Gulo*), and desmoglein 1 alpha (*Dsg1a*). (**E**) Expression of antigen-processing and -presentation genes in eTACs relative to other lymphoid cell populations after median-centered normalization to the expression of all genes in each array. (**F**) Global expression profile similarity of eTACs (left) and mTECs (right) to other relevant cell types based on Pearson correlation values calculated for population-specific centroids.

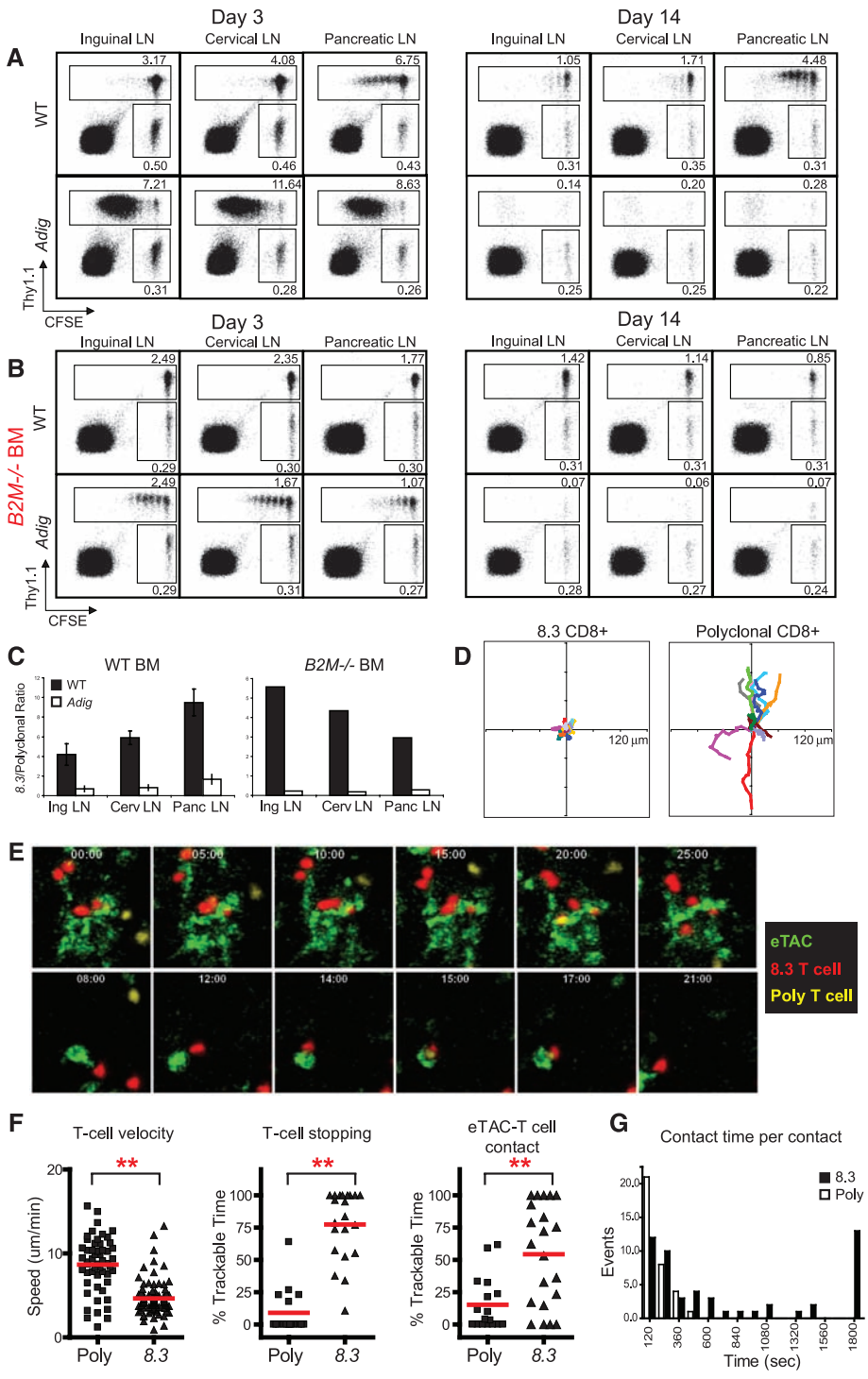

Fig. 4. eTACs directly interact with autoreactive lymphocytes and mediate deletional tolerance. (**A**) Flow cytometry of CFSE-labeled and adoptively cotransferred *8.3* $CD8^+$ T cells (Thy1.1) and polyclonal $CD8^+$ T cells (Thy 1.2). Cells were harvested at day 3 (left) and day 14 (right) after transfer (**B**) Adoptive transfer of the same donor populations as (A) into lethally irradiated wild-type (top) and *Adig* (bottom) recipients reconstituted with $\beta 2M^{-/-}$ bone marrow. (**C**) Quantitation of antigen-specific deletion after adoptive transfer at day 14 in (A) and (B), showing the ratio of *8.3* to polyclonal $CD8^+$ T cells in wild-type (black) and *Adig* (white) NOD recipients. Bars are representative of at least three mice each. (**D** to **G**) Two-photon imaging of *8.3* and polyclonal $CD8^+$ T cells in axillary lymph nodes 4 hours after adoptive transfer into *Adig* NOD recipients. (D) 10-min displacement analysis of all *8.3* $CD8^+$ T cell tracks (left) and polyclonal $CD8^+$ T cell tracks (right). (E) Representative images of interaction between *8.3* $CD8^+$ T cells (red), polyclonal $CD8^+$ T cells (yellow) and eTACs (green). (F) Average T cell track speed (left), percent of time in which a T cell is stopped (middle), and percent of time in which a T cell is making contact with an eTAC (right) among polyclonal (Poly) and *8.3* (*8.3*) CD8 T cells. $^{**}P < 0.001$. (G) Histogram displaying the duration of individual T cell–eTAC interaction times per contact for polyclonal (black bars) and *8.3* (white bars) $CD8^+$ T cells.

modest levels of TSA expression and *Aire*-dependent gene up-regulation in eTACs (approximately twofold). However, it is notable that similar analyses of *Aire*-expressing mTECs have demonstrated that TSAs are expressed at low levels in these cells (*2*), but even this low level of expression has proven critical for the maintenance of immune tolerance (*4*, *23*). Our findings suggest that eTACs may represent a safety net within the entire immunologic periphery, which functions to screen out naïve autoreactive T cell clones that escape thymic negative selection. Finally, we speculate that eTACs may play an increasingly important role with advancing age, as the thymus involutes and the burden of maintaining self-tolerance shifts to the periphery.

References and Notes

1. K. M. Smith, D. C. Olson, R. Hirose, D. Hanahan, *Int. Immunol.* **9**, 1355 (1997).
2. J. Derbinski, A. Schulte, B. Kyewski, L. Klein, *Nat. Immunol.* **2**, 1032 (2001).
3. J. Derbinski *et al.*, *J. Exp. Med.* **202**, 33 (2005).
4. M. S. Anderson *et al.*, *Science* **298**, 1395 (2002).
5. A. Liston, S. Lesage, J. Wilson, L. Peltonen, C. C. Goodnow, *Nat. Immunol.* **4**, 350 (2003).
6. C. Ramsey *et al.*, *Hum. Mol. Genet.* **11**, 397 (2002).
7. K. Nagamine *et al.*, *Nat. Genet.* **17**, 393 (1997).
8. Finnish-German APECED Consortium, *Nat. Genet.* **17**, 399 (1997).
9. J. W. Lee *et al.*, *Nat. Immunol.* **8**, 181 (2007).
10. M. Halonen *et al.*, *J. Histochem. Cytochem.* **49**, 197 (2001).
11. F. X. Hubert *et al.*, *J. Immunol.* **180**, 3824 (2008).
12. W. Yu *et al.*, *Science* **285**, 1080 (1999).
13. Materials and methods are available as supporting material on *Science* Online.
14. M. Nagata, P. Santamaria, T. Kawamura, T. Utsugi, J. W. Yoon, *J. Immunol.* **152**, 2042 (1994).
15. B. Han *et al.*, *J. Clin. Invest.* **115**, 1879 (2005).
16. S. M. Lieberman *et al.*, *Proc. Natl. Acad. Sci. U.S.A.* **100**, 8384 (2003).
17. I. Jarchum, L. Nichol, M. Trucco, P. Santamaria, T. P. Dilorenzo, *Clin. Immunol.* **127**, 359 (2008).
18. D. Gray, J. Abramson, C. Benoist, D. Mathis, *J. Exp. Med.* **204**, 2521 (2007).
19. M. S. Lin *et al.*, *J. Clin. Invest.* **105**, 207 (2000).
20. M. P. Marinkovich, T. B. Taylor, D. R. Keene, R. E. Burgeson, J. J. Zone, *J. Invest. Dermatol.* **106**, 734 (1996).
21. C. Kowal *et al.*, *Proc. Natl. Acad. Sci. U.S.A.* **103**, 19854 (2006).
22. M. Matloubian *et al.*, *Nature* **427**, 355 (2004).
23. J. DeVoss *et al.*, *J. Exp. Med.* **203**, 2727 (2006).

24. We thank J. Bluestone, A. Abbas, N. Killeen, and J. Cyster for helpful discussion. J.G. is funded by the UCSF/NIH Medical Scientist Training Program and the American Diabetes Association, J.D. by the Giannini Foundation, R.F. by the Larry L. Hillblom Foundation, and D.W. by a Dermatology Foundation Research Career Development Award. M.S.A. is supported by the Pew Scholars Program, the Sandler Foundation, and the Burroughs Wellcome Fund. This work was supported in part by NIH (to M.S.A.). The authors have no competing financial interests.

Supporting Online Material

www.sciencemag.org/cgi/content/full/321/5890/843/DC1
Materials and Methods
Figs. S1 to S5
Tables S1 and S2
References
Movies S1 to S6

21 April 2008; accepted 14 July 2008
10.1126/science.1159407